Long-lived complexes and signatures of chaos in ultracold K_{2}+Rb collisions

J. F. E. Croft, N. Balakrishnan, and B. K. Kendrick

Phys. Rev. A **96**, 062707 — Published 18 December 2017

DOI: 10.1103/PhysRevA.96.062707

Long-lived complexes and signatures of chaos in ultracold K_2+Rb collisions

J. F. E. Croft,[1] N. Balakrishnan,[1] and B. K. Kendrick[2]

[1] *Department of Chemistry, University of Nevada, Las Vegas, Nevada 89154, USA*
[2] *Theoretical Division (T-1, MS B221), Los Alamos National Laboratory, Los Alamos, New Mexico 87545, USA*

Lifetimes of complexes formed during ultracold collisions are of current experimental interest as a possible cause of trap loss in ultracold gases of alkali-dimers. Microsecond lifetimes for complexes formed during ultracold elastic collisions of K_2 with Rb are reported, from numerically-exact quantum-scattering calculations. Thermally averaged lifetimes are compared with those calculated using a simple density-of-states approach, which are shown to be reasonable. This validates the density-of-states approach and suggests that the formation of long-lived complexes is indeed the cause of observed experimental trap loss in ultracold alkali dimer systems. Long-lived complexes correspond to narrow scattering resonances which we examine for the statistical signatures of quantum chaos, finding that the positions and widths of the resonances are in good agreement with the Wigner-Dyson and Porter-Thomas distributions respectively.

I. INTRODUCTION

The ability to create ultracold atomic and molecular gases has engendered extraordinary progress in diverse areas of physics and chemistry. In few-body physics the first experimental observation of Efimov states was made in a gas of ultracold ceasium [1]; in many-body physics experimental observation of zero-temperature quantum phase transitions have been made in a gas of ultracold rubidium atoms trapped in an optical lattice [2]; in precision measurement the development of new atomic-clock technologies has used ultracold strontium trapped in an optical lattice [3]. What all these diverse applications have in common is that they take advantage of the exquisite precision and control uniquely attainable in the ultracold regime.

Ultracold molecules share the precision and control of ultracold atomic gases, while their richer internal structure and long-range anisotropic interactions open up an even more diverse range of applications. Cold and ultracold molecules have been used to study chemical reactions at their most fundamental level [4–8], measure the shape of the electron [9, 10], and perform precision spectroscopy of complex molecules [11]. There is a wide array of theory proposals for ultracold molecular samples, which take advantage of the complexity of molecules relative to atoms, from studying novel quantum phases [12–14] to quantum information processing [15–18]. Such proposals rely on the ability to produce a stable ultracold molecular gas without significant loss.

The rich structure of molecules is however both a blessing and a curse. Trap loss has been found to be a limiting factor in ultracold molecule experiments with alkali dimers [19–22]. This loss persists even when the molecules are in their absolute ground-state and only elastic collisions are possible. One possible mechanism for this loss is the formation of long-lived complexes. Based on statistical arguments, Mayle *et al* have proposed that due to the high density-of-states (DOS) in such systems 4-body complexes can have lifetimes of order 1-10 ms [23, 24]. If these lifetimes are reasonable then this could explain the experimentally observed trap loss, which limits trap lifetime to the order of seconds. Lifetime estimates for 3-body alkali complexes formed in atom-dimer collisions using this DOS approach have been shown to be reasonable when compared to estimates from classical trajectory calculations [25]. So far, however, there has been no explicit experimental measurement or theory predication based on quantum calculations for such lifetimes.

Such complexes can also be considered a feature not a bug. They are expected to exhibit the Wigner-Dyson energy level statistics associated with quantum chaos. There has been recent interest in understanding the role of chaos in cold collisions [23–35]. Ultracold molecular collisions are complex and understanding them in chaotic terms could allow for the considerable insight gained in nuclear physics to be applied to ultracold atomic and molecular physics [36]. For example Mayle *et al* have developed a statistical scattering formalism which assumes the formation of chaotic complexes at short range [23, 24].

In this work we report explicit delay times for elastic K_2-Rb collisions, obtained from numerically-exact quantum-scattering calculations. Thermally averaged delay times are compared with lifetimes for the collision complex predicated by a simple DOS approach finding them to be reasonable and validating their use for other similar systems. We also examine the statistics of resonance positions and widths for the signatures of chaos finding that they are in good agreement with the Wigner-Dyson and Porter-Thomas distributions respectively.

II. METHODS

We use the atom-diatom scattering formalism as developed by Pack and Parker [37, 38]. The scattering calculations can broadly be split into three main steps: the numerical computation of 5D hyperspherical surface functions in the adiabatically-adjusting principle-axis hyperspherical (APH) coordinates in the short-range region and Delves hyperspherical coordinates (DC) in the long-range region; the log-derivative propagation of the

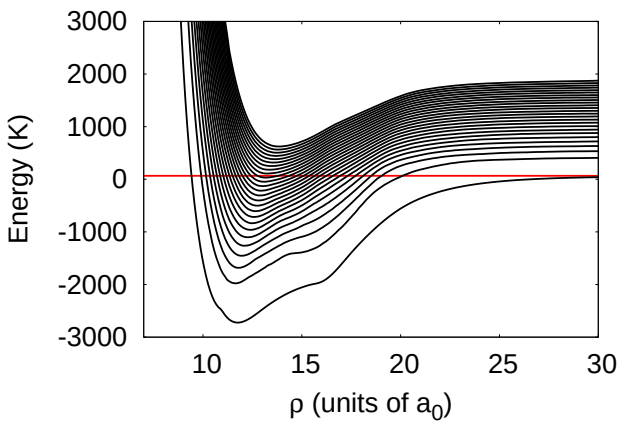

FIG. 1. The adiabatic potential curves for the KRbK complex at short hyperradius for even exchange symmetry. Only every 100th curve is shown due to the high DOS for this system. The horizontal red line corresponds to the $v = 0$ $j = 0$ threshold of K_2.

CC equation in these coordinates; finally, the asymptotic matching to ro-vibrational states in Jacobi coordinates.

The Hamiltonian for a triatomic system in hyperspherical coordinates is

$$H = -\frac{\hbar^2}{2\mu\rho^5}\frac{\partial}{\partial\rho}\rho^5\frac{\partial}{\partial\rho} + \frac{\hat{\Lambda}^2}{2\mu\rho^2} + V\,, \qquad (1)$$

where $\mu = \sqrt{m_A m_B m_C/(m_A + m_B + m_C)}$ is the three-body reduced mass, $\hat{\Lambda}$ is the grand angular momentum operator and V is the potential energy surface as a function of the chosen hyperspherical coordinates.

In the short-range region APH coordinates (ρ, θ, ϕ) are used as they evenhandedly treat all three arrangement channels, τ, of an A+BC system. For each ρ the surface functions are computed which are eigen-solutions of the Hamiltonian $H^{5D} = \hat{\Lambda}^2/(2\mu\rho^2) + 15\hbar^2/(2\mu\rho^2) + V(\rho,\theta,\phi)$ for a given total angular momentum J, parity, and exchange symmetry. The 5D surface functions are functions of two internal coordinates θ and ϕ and three Euler angles α, β, and γ to orient the molecule in space. The size of the APH surface functions basis sets in θ and ϕ are determined by $l_{\max}$ and $m_{\max}$ respectively [38]. In this work the short-range region is from $\rho = 8.0\ a_0$ to $38.15\ a_0$, where a_0 is the Bohr radius ($a_0 = 0.0529177$ nm). This region is further subdivided into six, with increasing $l_{\max}$ and $m_{\max}$ to ensure converged surface functions. These regions are $8.0\ a_0 \le \rho < 11.33\ a_0$, $11.33\ a_0 \le \rho < 16.87\ a_0$, $16.87\ a_0 \le \rho < 18.82\ a_0$, $18.82\ a_0 \le \rho < 22.74\ a_0$, $22.74\ a_0 \le \rho < 32.21\ a_0$, and $32.21\ a_0 \le \rho < 38.15\ a_0$ with $l_{\max} = 103, 117, 123, 149, 169, 189$ and $m_{\max} = 206, 234, 246, 298, 338, 378$, respectively. For $J = 0$ this leads to 5D surface function matrices of dimension 42 952, 55 342, 61 132, 89 550, 115 090, and 143 830. Explicit diagonalization of such large matrices is not computationally tractable so we use the sequential diagonalization truncation technique [39, 40] to reduce the dimension. The matrices are sparse and the implicitly restarted lanczos method [41] is used to compute only the lowest 2543 surface functions for even exchange symmetry and parity needed for the log-derivative propagation. These surface functions are computed on a logarithmic grid in ρ with 157 sectors. This approach is capable of fully representing the complex collision dynamics of three atoms at short range which is the source of the long lifetimes predicted by Mayle *et al.*

Outside the short-range region, where the three-body interaction has nearly decayed to zero, Delves hyperspherical coordinates (ρ, θ_τ, γ_τ) are used. The hyperradius is the same as in APH coordinates but the hyperangles are defined differently and depend on the arrangement channel τ. The hyper angle γ_τ is the angle between S_τ and s_τ and $\theta_\tau = \arctan(s_\tau/S_\tau)$ where S_τ and s_τ are mass-scaled Jacobi coordinates for the atom-molecule center-of-mass separation and the diatom separation respectively [42, 43]. Delves coordinates are used from $\rho = 38.15$ a$_0$ to $\rho_{max} = 174.95$ a$_0$ and surface functions are computed on a linear grid with 456 sectors. The number of basis functions is determined by an energy cutoff of 0.3 eV relative to the minimum energy of the asymptotic K_2 diatomic potential. A one-dimensional Numerov method is used to compute the adiabatic surface functions.

The log-derivative matrix is propagated to $\rho_{\max}$ using the method of Johnson [44]. Only $J = 0$, even exchange symmetry, and even parity are required as here we are interested in ultracold collisions where the initial channel is K_2 $j = 0$. In the APH region the propagation includes 2543 channels of which over 35% are closed at all ρ. The DC region only requires 423, as many of the channels locally open at short range have become strongly closed. Consequently the long-range propagation takes a negligible time compared to the short-range as the computational cost scales as the number of channels cubed. At $\rho = \rho_{\max}$, the DC wave functions are matched to asymptotic channel functions corresponding to ro-vibrational levels of the KRb and K_2 molecules, defined in Jacobi coordinates. This includes vibrational levels up to 2 for KRb and 5 for K_2 with rotational levels up to a maximum of 68 and 93 respectively.

We emphasize that while in this work we are primarily interested in elastic scattering this reactive formalism is in fact required as many of the channels open at short hyperradius correspond asymptotically to closed-channel configurations with a bound KRb dimer. The lowest 2500 adiabatic potential curves are shown in figure 1 where the high DOS which leads to the complex short-range dynamics can easily be seen. All calculations are for total angular momentum $J = 0$ even parity and even identical-particle exchange symmetry. Coupling of the orbital angular momenta with both the electron and nuclear spins is omitted. For non-zero J, the computational cost is prohibitive scaling as $\mathcal{O}((J+1)^3)$, even when we take ad-

vantage of parity and exchange symmetries. Fortunately, we are primarily interested in the ultracold regime where only s-wave collisions contribute (that is, only $J = 0$ is required for K_2 in the ground rotational state $j = 0$). An *ab initio* ground-state potential energy surface was used which accurately accounts for the long-range dispersion behavior, for details see [29].

III. RESULTS

A. Long-lived complexes

The long lifetimes predicted for complexes in ultracold alkali-dimer collisions are due to two main factors. Firstly deep potentials and heavy atoms lead to a high DOS, classically this corresponds to many ro-vibrational degrees-of-freedom for the energy to distribute into. Secondly few exit channels mean the complex spends a long time exploring these degrees-of-freedom before finding a way out. These concepts are codified by Rice-Ramsperger-Kassel-Marcus (RRKM) theory [45–47]. RRKM theory predicts a lifetime given by

$$\tau = \frac{2\pi\hbar\rho}{N_o}, \tag{2}$$

where ρ is the DOS and N_o is the number of energetically allowed exit channels. The RRKM lifetime originated in transition state theory however it has been used by Mayle *et al* as a way to estimate lifetimes in ultracold molecular collisions [23, 24]. The beauty of equation 2 is its simplicity, only an estimate of the DOS and the number of open channels is needed to calculate a complex lifetime at a given energy.

We proceed to calculate the lifetime of a KRbK complex, formed in elastic K_2+Rb collisions, by following the method detailed by Mayle *et al* for estimating ρ [23]. For the K_2 dimer potential we use a Lennard-Jones potential with C_6 and D_e taken from [48]. To obtain the C_6 and D_e required for the Lennard-Jones K_2-Rb potential we use the C_6 and D_e for KRb taken from [49] and assume the three-body potential is pairwise additive, with C_6 and D_e chosen to be double the atom + atom value for the atom + dimer potential. In this way the choice of C_6 used to estimate the DOS is the same as the C_6 used in the scattering calculations. The 1d-Schrödinger equation was solved using the Fourier-grid-Hamiltonian method [50, 51]. In order to compare to our scattering calculations we make a couple of changes to the method given in reference [23]. In that model each channel is defined by the asymptotic ro-vibrational quantum numbers j and v and the quantum number L for the end-over-end angular momentum of the atom and the molecule, and their projection quantum numbers M_L and m_j. The DOS is then estimated for a given total angular momentum J and projection M. To account for the identical particle symmetry we only include even rotational levels for K_2. We also only include channel quantum numbers

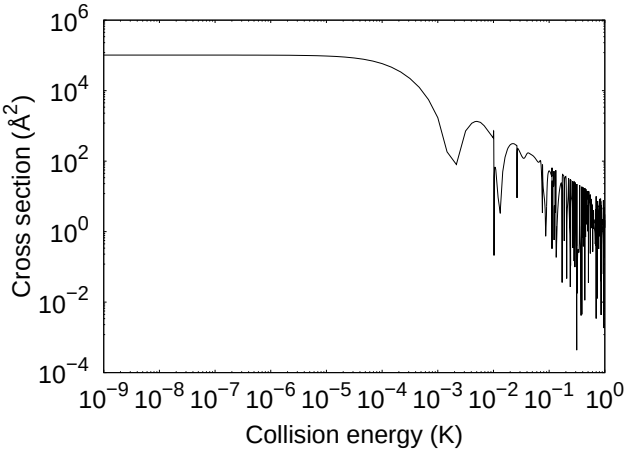

FIG. 2. Elastic cross-section for s-wave collisions of $K_2(v = 0, j = 0)$ with Rb as a function of energy ($J = 0$).

j, v and L (and not M_L and M_j) as our scattering calculations are field free and channels with different projection quantum numbers will be degenerate. Using this approach the estimate for ρ is 28 K^{-1} which gives a complex lifetime of 1.3 ns. If we instead include projection quantum numbers we find a DOS of 3 mK^{-1} and a complex lifetime of 167 ns, around 2 orders of magnitude longer. This large difference is due to channels with rotational quantum numbers j and L as high as 246 which are still locally open at short range and contribute to the DOS. For example taking $J = 0$, $M = 0$ as we have here $j = L$ and there are $2j + 1$ combinations of M_L and M_j consistent with $M = 0$ all of which contribute to the DOS.

The lifetime estimate given by equation 2 is the average lifetime, and assumes the average is taken over a wide enough energy range to include multiple resonances [24]. Assuming a thermal distribution, equation 2 is therefore valid when the temperature is above the mean spacing of resonances. Figure 2 shows the elastic cross-section for collisions of $K_2(v = 0, j = 0)$ with Rb as a function of energy, for total angular momentum $J = 0$. It is seen that there is a forest of narrow resonances starting at about 10 mK, each of which corresponds to a long-lived KRbK complex. The zero-energy cross-section gives a scattering length of 90 Å which compares well to the average scattering length of 47 Å obtained from the C_6 coefficient [52].

In order to assess the validity of the DOS lifetime estimates we compute explicit lifetimes of the collision complex from Smith's $\mathbf{Q}$ matrix,

$$\mathbf{Q} = i\hbar\mathbf{S}\frac{\partial\mathbf{S}^\dagger}{\partial E}. \tag{3}$$

The eigenvalues of $\mathbf{Q}$ are the time delays between a collision with and without a potential [53, 54]. The trace of $\mathbf{Q}$ is therefore the sum of the delay times for each channel. The matrix $\mathbf{Q}$ can be obtained directly by propagating the energy-derivative of the log-derivative matrix,

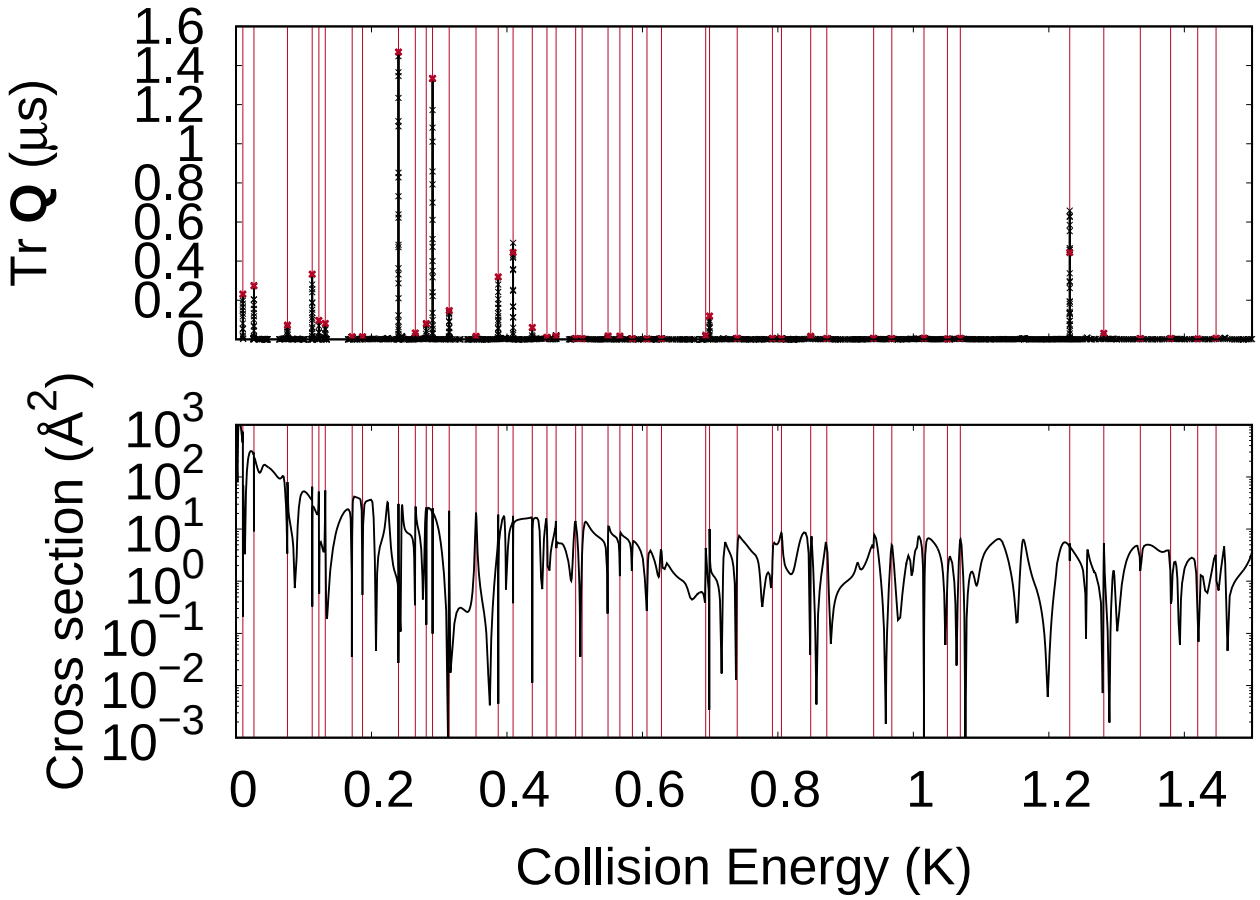

FIG. 3. Upper panel: Tr($\mathbf{Q}$) as as a function of collision energy. Lower panel: elastic cross-section for collisions of $K_2(v = 0, j = 0)$ with Rb as a function of energy. The vertical red lines mark the resonance positions while the red crosses show the resonance lifetimes. The K_2 $v = 0, j = 2$ channel becomes open at 0.47 K. The elastic cross-section is the same as shown in figure 2.

which can be done efficiently at the same time as the log-derivative propagation [55]. This allows for the direct calculation of $\mathbf{Q}$ from the energy derivatives $\mathbf{S}$. This approach has been extensively used to compute Smith delay times in a variety of systems and contexts [56–58].

Figure 3 plots Tr($\mathbf{Q}$) as a function of energy along with the cross-section on the same energy grid. It is clearly seen that there are many resonances with lifetimes as long as microseconds. The lifetimes are computed on a energy grid with over 1600 points. The small gaps seen in the energy grid are regions where the delay time is negative. Smith time delays are the difference between the time for a collision and the time for a collision without a potential, we refer to the latter as the background collision time. This definition leads to negative delay times away from resonances as the background collision time is large due to the lack of an attractive potential, compared to the collision time with a potential, especially at low collision energies. Following [57] we fit each of the resonances to a Breit-Wigner form

$$Q(E) = 2\hbar \frac{\Gamma_r/2}{[(E_r - E)^2 + (\Gamma_r/2)^2]}, \tag{4}$$

where E_r and Γ_r are the resonance energy and width respectively. This allows us to unambiguously assign a lifetime of $\frac{4\hbar}{\Gamma_r}$ to each resonance seen in figure 3. The position and lifetime for each resonance are shown in figure 3 as solid red vertical lines and red dots respectively. The lifetimes for the 10 narrowest resonances are given in Table I.

We now proceed to assess the validity of the DOS model for this kind of system as well as the experimental implications of these results. We find excellent agreement with the DOS model which predicted $\rho = 28$ K^{-1} while we find 44 resonances in a 1.5 K energy range which gives 29 K^{-1}. This close agreement is probably fortuitous given the approximations made in the DOS approach, however it does clearly show that such estimates are reasonable. Figure 4 compares the thermally

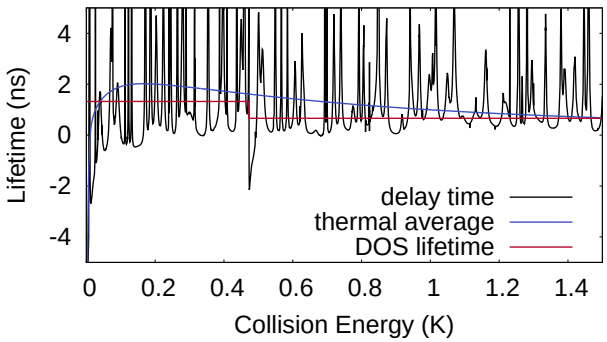

FIG. 4. Comparison of the lifetime of KRbK collision complex as a functions of energy from three different approaches: explicit delay time, thermally-averaged delay time, and the DOS estimate. The Smith delay time is the same as shown in the upper panel of figure 3.

averaged Smith delay time with the DOS lifetime predicted by equation 2. It is seen that except at very low energies where the negative background gives unphysical results the agreement is excellent. The DOS lifetime is only valid in regimes where that average is taken over an energy range which includes many resonances, which corresponds experimentally to temperatures T much greater than the mean resonance spacing ($T \gg 1/\rho$). This suggests that in principle it is always possible to avoid the formation of long-lived complexes by cooling to lower temperatures. Indeed for atom+dimer alkali collisions the DOS is estimated to be around 1-10 mK^{-1} [23], which suggests that sticking will not be an issue at temperatures below 1 mK. However for alkali dimer+dimer systems the DOS is estimated to be around 1-10 nK^{-1} [24], which would require temperatures below 1 nK. This is orders of magnitudes lower than temperatures at which trap loss has been seen in ultracold gases of alkali dimers which suggests that long-lived 4-body complexes are indeed the cause of the observed loss.

Energy (K)	Lifetime (μs)	Width (μK)
0.24	1.47	20.80
0.29	1.33	22.90
0.41	0.44	68.75
1.23	0.44	68.83
0.11	0.33	91.63
0.39	0.32	95.72
0.03	0.27	111.65
0.01	0.23	132.01
0.31	0.15	207.77
0.70	0.12	256.15

TABLE I. Position, lifetime and width of the 10 narrowest resonances.

B. Quantum chaos

Quantum-scattering calculations for collisions of ultracold molecules are extremely computationally expensive. Even though here we have presented results for only total angular momentum $J = 0$, even exchange symmetry and parity, included no spin or field effects the calculations still required over 300,000 hours of CPU time. It is possible that numerically exact quantum scattering calculations including all the effects omitted in these calculation will never be computationally tractable. As such statistical approaches offer an alternative way to attack such problems [23, 24, 27, 59, 60].

Atom-dimer ultracold collisions have been shown to be classically chaotic [25] and the analysis of short range adiabats of KRbK have been shown to exhibit the characteristics of quantum chaos [29]. While quantum systems cannot exhibit the non-linearity characteristic of classical chaos (in quantum mechanics operators are linear [61]) quantum analogs of classically chaotic systems do exhibit certain statistical signatures [62], such as Wigner-Dyson energy-level statistics [63, 64], Ericson fluctuations [65, 66], and Porter-Thomas resonance-width statistics [67].

We now proceed to examine the statistical distribution of resonance positions for evidence of quantum chaos. The distribution of scaled nearest-neighbor spacings for non-chaotic systems is given by the Poisson distribution, $\exp(-s)$, where small spacings predominate. However in quantum systems chaos manifests itself in the repulsion between energy levels [63], the distribution of scaled nearest-neighbor spacings is then given by a Wigner-Dyson distribution [64]. For Hamiltonians with time-reversal symmetry, such as we have here, the nearest-neighbor spacings are given by,

$$P_{\mathrm{wd}}(s) = \frac{\pi}{2} s \exp\left(-\frac{\pi}{4} s^2\right). \tag{5}$$

The upper panel of Figure 5 shows the distribution of scaled nearest-neighbor spacings between the 44 resonances shown in figure 3. While we have not found enough resonances to make a definitive statement as to whether this system exhibits quantum chaos we do clearly see the repulsion between neighbouring resonances characteristic of quantum chaos.

The degree of repulsion between the resonances can be quantified by the Brody parameter [68, 69]. The Brody parameter is itself not physically meaningful, rather is defined to smoothly interpolate between the Poisson distribution and the Wigner-Dyson distribution,

$$\begin{aligned} P_{\mathrm{b}}(s) &= A s^{\eta} \exp\left(-\alpha s^{\eta+1}\right), \\ A &= (\eta+1)\alpha, \\ \alpha &= \Gamma\left(\frac{\eta+2}{\eta+1}\right)^{\eta+1}, \end{aligned} \tag{6}$$

where η is the Brody parameter. For $\eta = 0$ the distribution reduces to P_{p} and for $\eta = 1$ it reduces to P_{wd}.

Performing a least-squares fit of equation 6 to the data shown in the upper panel of figure 5 we obtain a Brody parameter of $\eta = 0.78 \pm 0.04$. Despite the relatively small number of resonances found this value is clearly suggestive of a significantly, though not fully, chaotic system. In a previous work on the collisions of Li with CaH it was found that the Brody parameter was sensitive to scaling of the potential [28]. Unfortunately we are unable to explore this dependence in this work due to the high computational cost of our calculations, though we note that the Brody parameter for the short-range adiabats for this system has previously been shown to be insensitive to such a scaling [29].

We now move on to examine another statistical characteristic of chaos in quantum systems, the Porter-Thomas distribution of resonance widths [67]. Porter-Thomas statistics describe the distribution of velocity-independent reduced widths, $\Gamma_n^0 = \Gamma_n / E_0^{\frac{1}{2}}$. The scaled reduced widths, $\Gamma_n^0 / \langle \Gamma_n^0 \rangle$, for chaotic systems follow the chi-squared distribution χ_k^2 with degree $k = 1$. The lower panel of Figure 5 shows the distribution of reduced widths for the resonances shown in figure 3. Despite the relatively small statistical sample we clearly see broad agreement with the overall trend of the Porter-Thomas distribution towards resonances with smaller widths.

The signatures of chaos exhibited by the scattering is a consequence of the strong coupling between all channels allowed by conservation of energy and angular momentum. This gives important insight into the nature of the short-range dynamics of this system and shows that even in elastic collisions both inelastic and reactive channels play an important role in the dynamics. The DOS approach relies precisely on this assumption (that the entire phase space allowed by conservation of energy and angular momentum is in fact explored by the collision complex) which explains the good agreement of the DOS model with the scattering results we have found for this system. The chaotic nature of the complex at short hyperradius is not specific to collisions of K_2 with Rb however which suggests that DOS predications for other ultracold atom + dimer and dimer + dimer elastic collisions involving heavy alkali atoms are also reasonable.

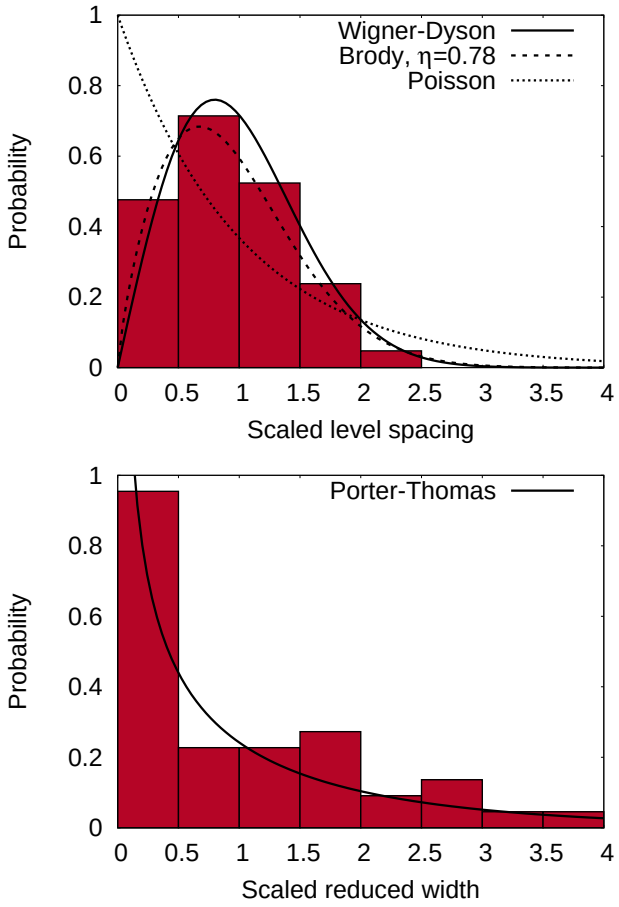

FIG. 5. Distribution of scaled nearest-neighbor spacings (upper panel) and scaled reduced widths (lower panel) for scattering resonances, shown as solid red lines in figure 3.

IV. CONCLUSIONS

We have examined ultracold elastic K_2-Rb collisions and reported explicit lifetimes for long-lived complexes formed during the collision process, finding that such lifetimes can be of the order of microseconds. Such long lifetimes are due to the high DOS for this system combined with the strong coupling between inelastic and reactive channels which are closed asymptotically but open at short range. Thermally averaged lifetimes were compared with those predicted using a simple DOS approach based on RRKM theory which are shown to be reasonable. This suggests that the formation of long-lived complexes is indeed the cause of observed experimental trap loss in ultracold alkali dimer systems.

Long-lived complexes correspond to narrow resonances in quantum scattering. We have analyzed the distribution of nearest-neighbor spacings and widths of these resonances and have found that they both exhibit the statistical signatures of quantum chaos. Quantum scattering calculations for collisions of ultracold molecules are extremely computationally expensive. It is possible that numerically-exact quantum-scattering calculations including all the effects of interest will never be computationally tractable. As such the chaotic nature of systems such as this suggests a statistical approach to tackling such problems could be fruitful.

In future work we intend to examine the effect of including the excited doublet state on the lifetimes. Including the excited state in the calculations will allow for the full treatment of the conical intersection and the possibility of long-lived quasi-bound states on the upper surface.

V. ACKNOWLEDGMENTS

We acknowledge C. Makrides, M. Li, and S. Kotochigova for helpful discussions. We acknowledge support from the US Army Research Office, MURI grant No. W911NF-12-1-0476 (N.B.), and the US National Science Foundation, grant No. PHY-1505557 (N.B.). BKK acknowledges that part of this work was done under the auspices of the US Department of Energy, Project No. 20170221ER of the Laboratory Directed Research and Development Program at Los Alamos National Laboratory. Los Alamos National Laboratory is operated by Los Alamos National Security, LLC, for the National Security Administration of the US Department of Energy under contract DE-AC52-06NA25396. JFEC gratefully acknowledges support from the ITAMP visitors program.

[1] T. Kraemer, M. Mark, P. Waldburger, J. G. Danzl, C. Chin, B. Engeser, A. D. Lange, K. Pilch, A. Jaakkola, H. C. Nägerl, and R. Grimm, Nature **440**, 315 (2006).
[2] M. Greiner, O. Mandel, T. Esslinger, T. W. Hänsch, and I. Bloch, Nature **415**, 39 (2002).
[3] B. Bloom, T. Nicholson, J. Williams, S. Campbell, M. Bishof, X. Zhang, W. Zhang, S. Bromley, and J. Ye, Nature **506**, 71 (2014).
[4] S. Ospelkaus, K.-K. Ni, D. Wang, M. H. G. de Miranda, B. Neyenhuis, G. Quéméner, P. S. Julienne, J. L. Bohn, D. S. Jin, and J. Ye, Science **327**, 853 (2010).
[5] S. Knoop, F. Ferlaino, M. Berninger, M. Mark, H.-C. Nägerl, R. Grimm, J. P. D'Incao, and B. D. Esry, Phys. Rev. Lett. **104**, 053201 (2010).
[6] J. Rui, H. Yang, L. Liu, D.-C. Zhang, Y.-X. Liu, J. Nan, Y.-A. Chen, B. Zhao, and J.-W. Pan, Nature Phys. **13**, 699 (2017).
[7] W. E. Perreault, N. Mukherjee, and R. N. Zare, Science **358**, 356 (2017).
[8] J. Wolf, M. Deiß, A. Krükow, E. Tiemann, B. P. Ruzic, Y. Wang, J. P. D'Incao, P. S. Julienne, and J. H. Denschlag, Science **358**, 921 (2017).
[9] J. J. Hudson, D. M. Kara, I. Smallman, B. E. Sauer, M. R. Tarbutt, and E. A. Hinds, Nature **473**, 493 (2011).
[10] J. Baron, W. C. Campbell, D. DeMille, J. M. Doyle, G. Gabrielse, Y. V. Gurevich, P. W. Hess, N. R. Hutzler, E. Kirilov, I. Kozyryev, B. R. O'Leary, C. D. Panda, M. F. Parsons, E. S. Petrik, B. Spaun, A. C. Vutha, and A. D. West, Science **343**, 269 (2014).
[11] B. Spaun, P. B. Changala, D. Patterson, B. J. Bjork, O. H. Heckl, J. M. Doyle, and J. Ye, Nature **533**, 517 (2016).
[12] A. Micheli, G. Pupillo, H. P. Büchler, and P. Zoller, Phys. Rev. A **76**, 043604 (2007).
[13] M. L. Wall and L. D. Carr, New J. Phys. **11**, 055027 (2009).
[14] W. Lechner, H.-P. Büchler, and P. Zoller, Phys. Rev. Lett. **112**, 255301 (2014).
[15] H. P. Büchler, E. Demler, M. Lukin, A. Micheli, N. Prokof'ev, G. Pupillo, and P. Zoller, Phys. Rev. Lett. **98**, 060404 (2007).
[16] A. André, D. DeMille, J. M. Doyle, M. D. Lukin, S. E. Maxwell, P. Rabl, R. J. Schoelkopf, and P. Zoller, Nature Phys. **2**, 636 (2006).
[17] S. F. Yelin, K. Kirby, and R. Côté, Phys. Rev. A **74**, 050301 (2006).
[18] D. DeMille, Phys. Rev. Lett. **88**, 067901 (2002).
[19] T. Takekoshi, L. Reichsöllner, A. Schindewolf, J. M. Hutson, C. R. Le Sueur, O. Dulieu, F. Ferlaino, R. Grimm, and H.-C. Nägerl, Phys. Rev. Lett. **113**, 205301 (2014).
[20] P. K. Molony, P. D. Gregory, Z. Ji, B. Lu, M. P. Köppinger, C. R. Le Sueur, C. L. Blackley, J. M. Hutson, and S. L. Cornish, Phys. Rev. Lett. **113**, 255301 (2014).
[21] J. W. Park, S. A. Will, and M. W. Zwierlein, Phys. Rev. Lett. **114**, 205302 (2015).
[22] M. Guo, B. Zhu, B. Lu, X. Ye, F. Wang, R. Vexiau, N. Bouloufa-Maafa, G. Quéméner, O. Dulieu, and D. Wang, Phys. Rev. Lett. **116**, 205303 (2016).
[23] M. Mayle, B. P. Ruzic, and J. L. Bohn, Phys. Rev. A **85**, 062712 (2012).
[24] M. Mayle, G. Quéméner, B. P. Ruzic, and J. L. Bohn, Phys. Rev. A **87**, 012709 (2013).
[25] J. F. E. Croft and J. L. Bohn, Phys. Rev. A **89**, 012714 (2014).
[26] J. L. Bohn, A. V. Avdeenkov, and M. P. Deskevich, Phys. Rev. Lett. **89**, 203202 (2002).
[27] V. V. Flambaum and J. S. M. Ginges, Phys. Rev. A **74**, 025601 (2006).
[28] M. D. Frye, M. Morita, C. L. Vaillant, D. G. Green, and J. M. Hutson, Phys. Rev. A **93**, 052713 (2016).
[29] J. F. E. Croft, C. Makrides, M. Li, A. Petrov, B. K. Kendrick, N. Balakrishnan, and S. Kotochigova, Nat. Commun. **8**, 15897 (2017).
[30] D. G. Green, C. L. Vaillant, M. D. Frye, M. Morita, and J. M. Hutson, Phys. Rev. A **93**, 022703 (2016).
[31] A. Frisch, M. Mark, K. Aikawa, F. Ferlaino, J. L. Bohn, C. Makrides, A. Petrov, and S. Kotochigova, Nature **507**, 475 (2014).
[32] T. Maier, H. Kadau, M. Schmitt, M. Wenzel, I. Ferrier-Barbut, T. Pfau, A. Frisch, S. Baier, K. Aikawa, L. Chomaz, M. J. Mark, F. Ferlaino, C. Makrides, E. Tiesinga, A. Petrov, and S. Kotochigova, Phys. Rev. X **5**, 041029 (2015).
[33] T. Maier, I. Ferrier-Barbut, H. Kadau, M. Schmitt, M. Wenzel, C. Wink, T. Pfau, K. Jachymski, and P. S. Julienne, Phys. Rev. A **92**, 060702 (2015).
[34] B. C. Yang, J. Pérez-Ríos, and F. Robicheaux, Phys. Rev. Lett. **118**, 154101 (2017).
[35] K. Jachymski and P. S. Julienne, Phys. Rev. A **92**, 020702 (2015).
[36] H. A. Weidenmüller and G. E. Mitchell, Rev. Mod. Phys. **81**, 539 (2009).
[37] R. T. Pack and G. A. Parker, J. Chem. Phys. **87**, 3888 (1987).
[38] B. K. Kendrick, R. T. Pack, R. B. Walker, and E. F. Hayes, J. Chem. Phys. **110**, 6673 (1999).
[39] Z. Bačić, R. Whitnell, D. Brown, and J. Light, Computer Physics Communications **51**, 35 (1988).
[40] Z. Bačić, J. Kress, G. Parker, and R. Pack, J. Chem. Phys. **92**, 2344 (1990).

[41] D. C. Sorensen, SIAM Journal on Matrix Analysis and Applications **13**, 357 (1992).
[42] L. Delves, Nuclear Physics **9**, 391 (1958).
[43] L. Delves, Nuclear Physics **20**, 275 (1960).
[44] B. R. Johnson, J. Comput. Phys. **13**, 445 (1973).
[45] R. A. Marcus, J. Chem. Phys. **20**, 352 (1952).
[46] R. A. Marcus, J. Chem. Phys. **20**, 355 (1952).
[47] R. D. Levine, *Molecular Reaction Dynamics* (Cambridge University Press, 2005).
[48] S. Falke, H. Knöckel, J. Friebe, M. Riedmann, E. Tiemann, and C. Lisdat, Phys. Rev. A **78**, 012503 (2008).
[49] A. Pashov, O. Docenko, M. Tamanis, R. Ferber, H. Knöckel, and E. Tiemann, Phys. Rev. A **76**, 022511 (2007).
[50] G. G. Balint-Kurti, R. N. Dixon, and C. C. Marston, Int. Rev. Phys. Chem. **11**, 317 (1992).
[51] C. C. Marston and G. G. Balint-Kurti, J. Chem. Phys. **91**, 3571 (1989).
[52] G. F. Gribakin and V. V. Flambaum, Phys. Rev. A **48**, 546 (1993).
[53] F. T. Smith, Phys. Rev. **118**, 349 (1960).
[54] F. T. Smith, in *Kinetic Processes in Gases and Plasmas*, edited by A. Hochstim (Academic Press, 1969) pp. 257 – 280.
[55] R. B. Walker and E. F. Hayes, J. Chem. Phys. **91**, 4106 (1989).
[56] B. Kendrick and R. T. Pack, Chem. Phys. Lett. **235**, 291 (1995).
[57] B. Kendrick and R. T. Pack, J. Chem. Phys. **104**, 7502 (1996).
[58] G. Guillon and T. Stoecklin, J. Chem. Phys. **130**, 144306 (2009).
[59] M. L. González-Martínez, O. Dulieu, P. Larrégaray, and L. Bonnet, Phys. Rev. A **90**, 052716 (2014).
[60] J. F. E. Croft and J. L. Bohn, Phys. Rev. A **91**, 032706 (2015).
[61] J. Von Neumann, *Mathematical foundations of quantum mechanics*, 2 (Princeton university press, 1955).
[62] O. Bohigas, M. J. Giannoni, and C. Schmit, Phys. Rev. Lett. **52**, 1 (1984).
[63] E. P. Wigner, Annals of Mathematics **53**, 36 (1951).
[64] F. J. Dyson, Journal of Mathematical Physics **3**, 140 (1962).
[65] T. Ericson, Phys. Rev. Lett. **5**, 430 (1960).
[66] T. Ericson, Annals of Physics **23**, 390 (1963).
[67] C. E. Porter and R. G. Thomas, Phys. Rev. **104**, 483 (1956).
[68] T. A. Brody, Lettere al Nuovo Cimento (1971-1985) **7**, 482 (1973).
[69] T. A. Brody, J. Flores, J. B. French, P. A. Mello, A. Pandey, and S. S. M. Wong, Rev. Mod. Phys. **53**, 385 (1981).